

# THE USE OF ULTRA-FAST RESPONSE ON-BOARD EXHAUST GAS ANALYZERS WITH ENHANCED SPATIAL AND TEMPORAL RESOLUTION FOR ACCURATE DEPOSITION MEASUREMENTS OF ROAD TRAFFIC POLLUTANTS

*Martin Irwin<sup>1</sup>, Mark S Peckham<sup>1</sup>, Harry Bradley<sup>1</sup>, Matthew Duckhouse<sup>1</sup>*

<sup>1</sup>Cambustion Ltd. Cambridge CB1 8DH, United Kingdom

**Abstract:** Accurate concentrations and locations of vehicle gaseous pollutants have been measured from a Euro 5 Diesel vehicle using on-board ultra-fast-response exhaust gas analyzers. The concentration data was measured simultaneous to high-resolution GPS location, and resulting pollution "hot spots" have been identified and plotted on satellite images. The results showed that transients associated with the negotiation of speed bumps, traffic lights, and other accelerations produced concentrations of NO<sub>x</sub> often exceeding 1,000 ppm. Such high concentrations, when combined with the exhaust mass flow, contributed to many hundreds of mg over just a few metres. This was particularly true of speed bumps where the enhanced time and space resolution identified the position and concentration of the pollutant cloud to within a few metres. It is anticipated that this technique, producing accurate source data, may be useful for both the modelling and measurement of pollutant dispersion after their initial release in to the atmosphere.

**Key words:** *Pollution, NO<sub>x</sub>, Fast Response Analyzer, Emissions, Dispersion.*

## INTRODUCTION

The growing concern over urban air quality (Chan & Yao, 2008) (Mayer, 1999) has led many cities to adopt widespread monitoring of their air quality using an array of roadside measurement equipment. One of the major sources of urban NO<sub>x</sub> pollution has been identified as road transport (Kagawa, 2002) with some countries announcing limitations on city access for internal combustion vehicles, including broader aims such as the electrification of the nations' vehicles. Typically the most recent air quality results from roadside monitoring stations are used to supply information to the public about the air quality associated with certain routes (Kings College London, 2013). This is published as a daily colour contour of the city's street map.

The modelling of the creation and dispersion of such pollution is of current interest but the accurate measurement of the generation mechanisms and sources of these emissions has, until now, been hampered by the relatively slow response of on-board emissions analyzers (typically a T<sub>10-90%</sub> rise time of several seconds). Most of a vehicle's emissions are caused during transient operation of the engine (for example, cold start, gear changes, accelerations and decelerations) (EU, 2016) Therefore, measurement equipment with response times sufficiently fast to accurately measure the "spike" of emissions (Collings & Willey, 1987) associated with a single gear change or rapid acceleration are required.

This paper presents data recorded with an ultra-fast response chemiluminescence analyzer (CLA) for NO<sub>x</sub> measurement with a T<sub>10-90%</sub> response of 10 milliseconds (which is sufficiently fast to accurately record and position emissions transients to within a few metres spatial resolution) via simultaneously-logged GPS (Department Of Defense, 2008).

## EXPERIMENT

Two candidate vehicles were chosen for this study, a Euro 5 compliant Diesel 7-seater with a 2.0 litre engine and a Euro 4 compliant 1.6 litre turbocharged gasoline direct injection passenger car.

A two-channel fast response CLA (Reavell, Collings, Peckham, & Hands, 1997) was adapted from its normal lab configuration to an on-board portable lay-out, powered by a 12 V battery. For the diesel vehicle, one channel of the fast CLA was configured for NO measurement and the 2nd channel for NO + NO<sub>2</sub> = NO<sub>x</sub> measurement. Both sample probes were positioned 200 mm inside the tailpipe of the vehicle. As it was anticipated that gasoline NO<sub>x</sub> emissions would be relatively low (NO<sub>x</sub> being mainly a byproduct of diesel-powered internal combustion engines) (Heywood, 1988), different sampling points were used for the GDI vehicle - to yield maximum possible time resolution, samples were taken upstream and downstream of the three-way catalyst. As both sample points were upstream of the muffler gaseous mixing was reduced.

Engine data was recorded from the vehicle's On-Board Diagnostics (OBD) port, allowing the exhaust mass flow to be measured at the same time as the emissions (essential for the derivation of gaseous emissions in terms of mass).

GPS data was also logged to the same data file. Further, a dashboard video camera was also used to record the driver's view.

Two routes around London and Cambridge were used to discover driving events which contribute significant NO<sub>x</sub> pollution, covering a multitude of real-world driving scenarios.

### RESULTS AND CONCLUSIONS

An overview map showing the Cambridge route (Figure 1) shows several points of high NO<sub>x</sub> deposition associated with cold start and transient features such as traffic lights, congestion and speed bumps (represented by the large black and red circles).

An advantage of the high resolution data is the ability to magnify areas of concern and accurately assess the location and concentration of the deposited pollutant. Some of the most significant features are described in detail below.

#### Speed bumps

The data from the diesel vehicle most clearly shows the location of speed bumps, due to the significantly higher NO<sub>x</sub> emissions associated with all accelerative phases (i.e. higher signal compared with gasoline measurements for the same test).

Figure 2 shows NO<sub>x</sub> and NO concentrations, and vehicle speed against time, with a spatial plot of NO<sub>x</sub> concentration on the right. The NO<sub>x</sub> and NO concentrations vary with vehicle speed over three subsequent speed bumps, labelled numerically on both the time-series and spatial plots.



**Figure 1.** An overview map showing NO<sub>x</sub> concentrations from a Diesel vehicle driven around Cambridge. Concentrations higher than 700 ppm per GPS point are circles coloured in black, at the largest diameter.

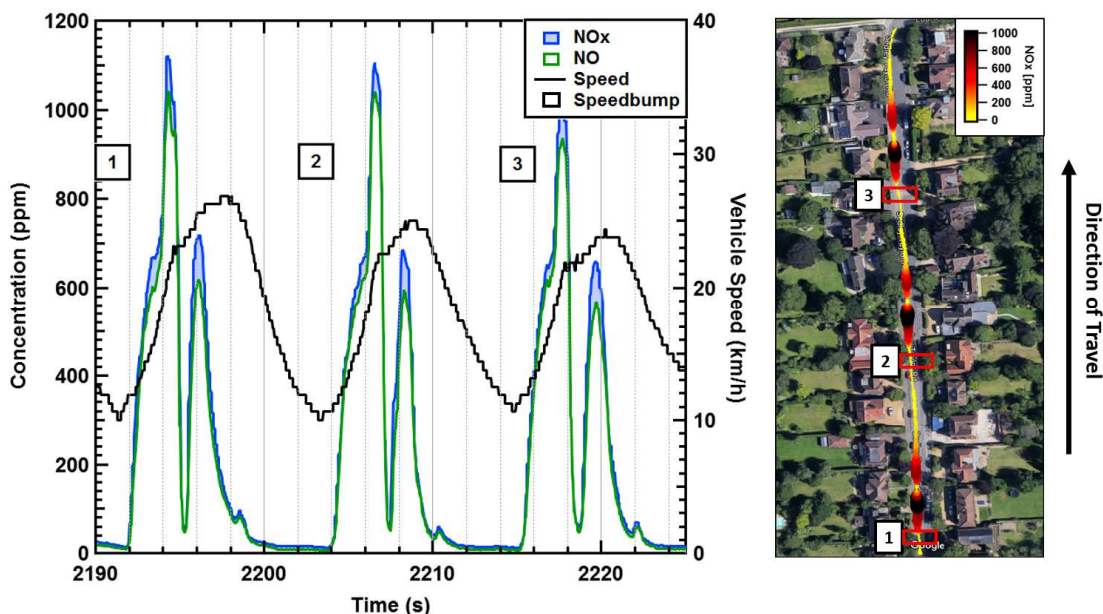


**Figure 2.** A graph showing gaseous concentrations of NO<sub>x</sub> and NO as a function of time whilst driving over three speed bumps in immediate succession. The plot on the right is a colour-contour plot superimposed on a satellite image.

The nature of speed bumps is to force the driver to slow significantly before accelerating back up to cruising speed, and are often located immediately outside schools or in residential areas as a safety measure. The largest emissions are again associated with acceleration – and this occurs immediately following each speed bump, as the driver accelerates back up towards the speed limit. The acceleration is briefly interrupted by a gear change, which is easily identified by the significant reduction in NO<sub>x</sub> concentration followed by an immediate sharp increase. The fast response time of this setup illustrates the high temporal resolution of each of these fast, transient features. Figure 3 shows the characteristics associated with a single speed bump.

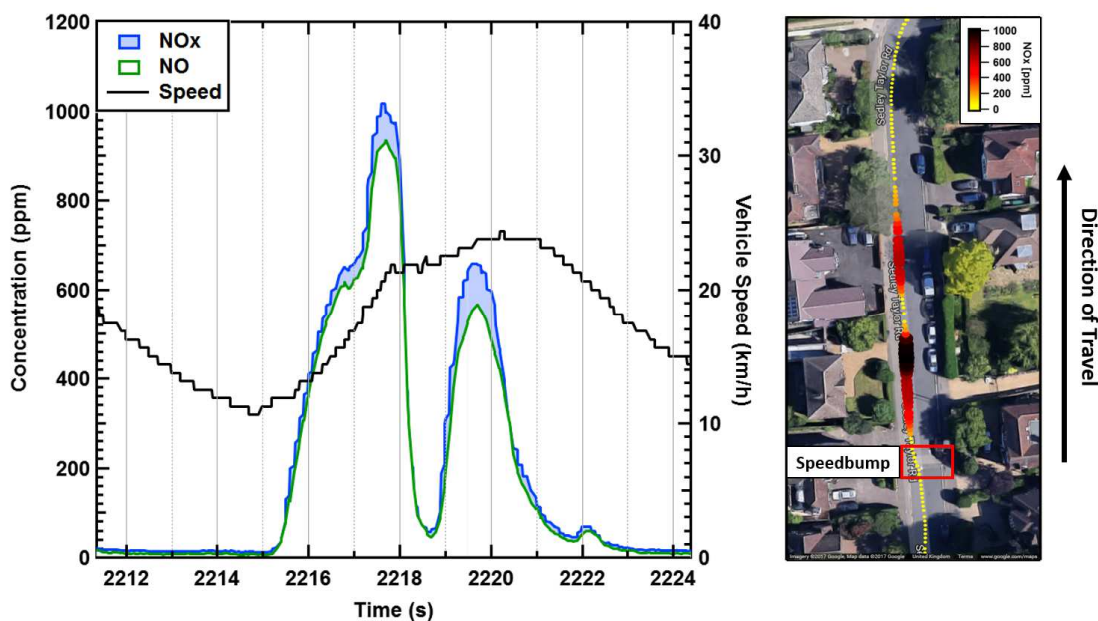


**Figure 3.** A graph showing gaseous concentrations of NO<sub>x</sub> and NO as a function of time for a single speed bump. The plot on the right is a colour-contour plot superimposed on a satellite image

Where decelerations are fairly sharp and fuel shut-off occurs, a sharp drop to close to zero is observed as there is no combustion producing NO<sub>x</sub> emissions. The inclusion of traffic calming measures such as speed bumps outside schools may reduce average vehicle road speeds, but appears to increase local pollution significantly.

### Traffic lights

Figure 4 shows the Diesel NO<sub>x</sub> and NO concentrations increasing from a 100 ppm baseline when stationary, associated with sustained lean operation of the engine during the idle period, to over 500 ppm during the accelerative phases (increased engine load) following each gear change after pulling away from the traffic lights. The right side of Figure 4 is a satellite view of central London, with NO<sub>x</sub> concentrations in ppm shown as a function of colour and size of the average value over each GPS point, for the route driven (driving direction indicated). The section of the drive shown on the left is contained within the white box.

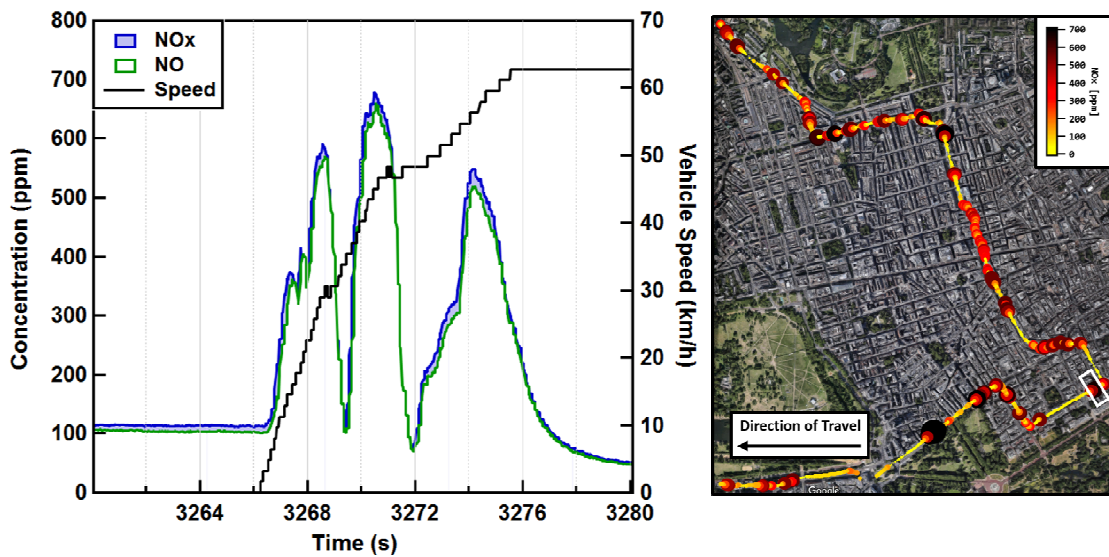


**Figure 4.** Measurement of NO<sub>x</sub>, NO and vehicle speed of a traffic light pull-away in central London, UK. The white box represents the spatial component of the graph data.

#### Motorway joining ramp

Figure 5 shows the data collected on the exit and entry slip road to a 70 mph dual-carriageway. On the left, a time series plot shows NO concentration from the EURO 4 Gasoline engine alongside vehicle speed. Phase 1 of the manoeuvre shows the deceleration off the dual-carriageway on approach to the first roundabout. As expected when slowing down, load on the engine is very low, and emissions are therefore minimal. Phase 2 shows the navigation of the first roundabout followed by an acceleration and gear-change between the two roundabouts. Immediately after the gear change, a very short duration spike of NO can be seen at 923 s. The magnitude of this spike is in excess of 2,200 ppm - a considerable emissions peak. Using much slower conventional PEMS equipment ( $T_{10-90\%} \sim 1s$ ), this highly time-resolved event would be significantly delayed, and smoothed out over a longer period. The inclusion of simultaneous GPS data identifies such emissions hot spots spatially.

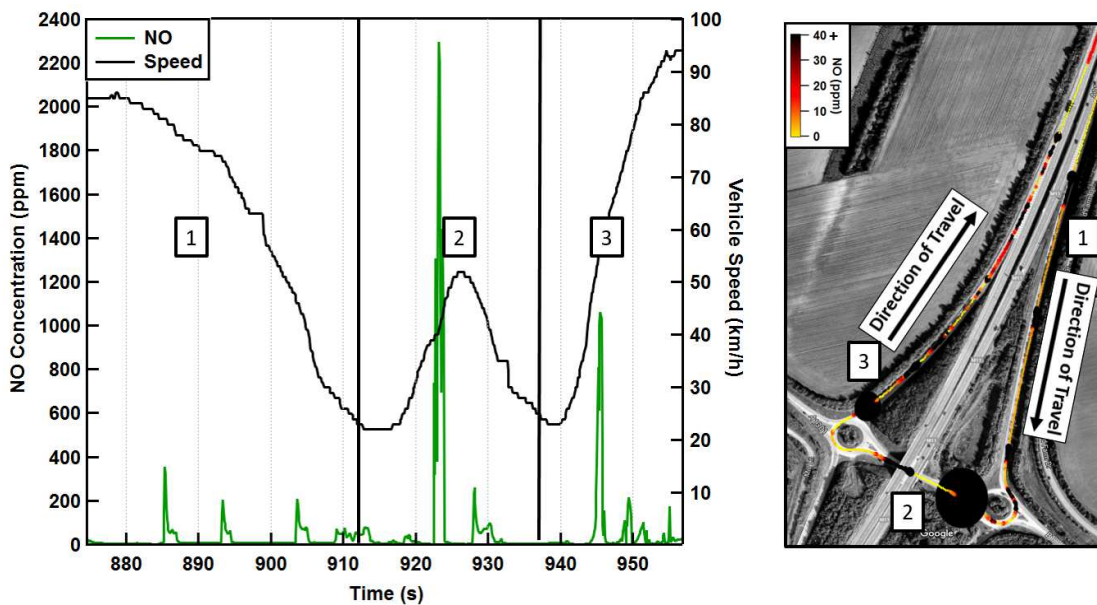


**Figure 5.** A plot showing NO concentrations from a petrol vehicle exiting and rejoining a motorway, with a colour-contour plot superimposed onto a satellite image on the right.

The scale of the spatial markers on Figure 5 correlate size and colour to average NO emissions at that time and location (i.e. values over 40 ppm are sized and coloured the same as at 40 ppm). A large black data point can be seen on the exit to the first roundabout to show the emissions at 923 s. A further spike in emissions was observed at the second roundabout, due to a second deceleration, followed by an acceleration. Phase 3 shows NO spikes correlating with gear changes and high load acceleration, as the vehicle joins the main dual-carriageway. The increased NO emissions with each high load event (after each gear change) are easily visualised on the GPS map plot on the right.

## CONCLUSIONS

Ultra-fast response engine exhaust emissions analyzers have been adapted for on-board vehicle use by reducing their size and power requirements below the original laboratory specification, resulting in an operating interval of at least two hours. Combined with OBD and GPS data, it is now possible, for the first time, to examine in detail transient features inherent in on-road driving and their associated emissions. NO<sub>x</sub> was chosen for this study as being one of the main urban air quality pollutants of interest, but fast response THC, CO and CO<sub>2</sub> analyzers can also be used in a similar manner. The analyzer's high sampling rate captures emissions events which would otherwise be lost or smoothed out when using conventional portable emissions equipment. Two vehicles, one diesel and one gasoline were tested over two routes, representative of legislated real driving emissions conditions. From the results areas of particular emissions concern such as traffic lights, motorway ramps, and speed bumps were examined in detail. These daily driving conditions all benefit from fast-gas measurement in terms of identifying under what engine conditions spikes in emissions occur, and the resultant emissions hot spots in terms of geographic location.

Future work will concentrate on the fast processing and presentation of such recorded data and also expanding the number of vehicle types tested.

## REFERENCES

- Chan, C. K., & Yao, X. (2008, January). Air pollution in mega cities in China. *Atmospheric Environment*. <https://doi.org/10.1016/j.atmosenv.2007.09.003>
- Collings, N., & Willey, J. (1987). Cyclically Resolved HC Emissions from a Spark Ignition Engine. <https://doi.org/10.4271/871691>
- Department Of Defense, U. S. . (2008). Global Positioning System Standard Positioning Service. *Www.Gps.Gov*, (September), 1–160. Retrieved from <http://www.gps.gov/technical/ps/2008-SPS-performance-standard.pdf>
- EU. COMMISSION REGULATION (EU) 2016/427 of 10 March 2016 amending Regulation (EC) No 692/2008 as regards emissions from light passenger and commercial vehicles (Euro 6), II Official Journal of the European Union § (2016). [https://doi.org/http://eur-lex.europa.eu/pri/en/oj/dat/2003/l\\_285/l\\_28520031101en00330037.pdf](https://doi.org/http://eur-lex.europa.eu/pri/en/oj/dat/2003/l_285/l_28520031101en00330037.pdf)
- Heywood, J. B. (1988). *Internal Combustion Engine Fundamentals*. (J. M. M. Anne Duffy, Ed.), *McGrawHill series in mechanical engineering* (1st ed., Vol. 21). McGraw-Hill Inc. <https://doi.org/10987654>
- Kagawa, J. (2002). Health effects of diesel exhaust emissions—a mixture of air pollutants of worldwide concern. *Toxicology*, 181–182, 349–353. [https://doi.org/10.1016/S0300-483X\(02\)00461-4](https://doi.org/10.1016/S0300-483X(02)00461-4)
- Kings College London. (2013). London Air Quality Network » Annual Pollution Maps. Retrieved August 4, 2017, from <https://www.londonair.org.uk/london/asp/annualmaps.asp>
- Ladommatos, N., & Rose, D. W. (1996). On the Causes of In-Cylinder Air-Fuel Ratio Excursions During Load and Fuelling Transients in Port-Injected Spark-Ignition Engines. <https://doi.org/10.4271/960466>
- Mayer, H. (1999). Air pollution in cities. In *Atmospheric Environment* (Vol. 33, pp. 4029–4037). [https://doi.org/10.1016/S1352-2310\(99\)00144-2](https://doi.org/10.1016/S1352-2310(99)00144-2)
- Rabinowitz, H., Siemund, S., Collin, T., & Campbell, B. (2007). Achieving EURO-III and EURO-IV with Ultra-Low Precious Metal Loadings. <https://doi.org/10.4271/2007-26-017>
- Reavell, K. S. J., Collings, N., Peckham, M., & Hands, T. (1997). Simultaneous Fast Response NO and HC Measurements from a Spark Ignition Engine. <https://doi.org/10.4271/971610>